

# Metabolic Response of Tomato Leaves Upon Different Plant–Pathogen Interactions<sup>†</sup>

M. Pilar López-Gresa,<sup>a,b</sup> Federica Maltese,<sup>b\*</sup> José María Bellés,<sup>a</sup> Vicente Conejero,<sup>a</sup> Hye Kyong Kim,<sup>b</sup> Young Hae Choi<sup>b</sup> and Robert Verpoorte<sup>b</sup>

## ABSTRACT:

**Introduction** – Plants utilise various defence mechanisms against their potential biotic stressing agents such as viroids, viruses, bacteria or fungi and abiotic environmental challenges. Among them metabolic alteration is a common response in both compatible and incompatible plant–pathogen interactions. However, the identification of metabolic changes associated with defence response is not an easy task due to the complexity of the metabolome and the plant response. To address the problem of metabolic complexity, a metabolomics approach was employed in this study.

**Objective** – To identify a wide range of pathogen (citrus exocortis viroid, CEVd, or *Pseudomonas syringae* pv. *tomato*)-induced metabolites of tomato using metabolomics.

**Methodology** – Nuclear magnetic resonance (NMR) spectroscopy in combination with multivariate data analysis were performed to analyse the metabolic changes implicated in plant–pathogen interaction.

**Results** – NMR-based metabolomics of crude extracts allowed the identification of different metabolites implicated in the systemic (viroid) and hypersensitive response (bacteria) in plant–pathogen interactions. While glycosylated gentisic acid was the most important induced metabolite in the viroid infection, phenylpropanoids and a flavonoid (rutin) were found to be associated with bacterial infection.

**Conclusions** – NMR metabolomics is a potent platform to analyse the compounds involved in different plant infections. A broad response to different pathogenic infections was revealed at metabolomic levels in the plant. Also, metabolic specificity against each pathogen was observed. Copyright © 2009 John Wiley & Sons, Ltd.

**Keywords:** *Solanum lycopersicum*; *Pseudomonas syringae*; Citrus exocortis viroid (CEVd); plant–pathogen interaction; NMR-based metabolomics

## Introduction

Over the years, many studies have been performed to analyse plant–pathogen interactions (reviewed by Mehta *et al.*, 2008). Plants have developed a number of strategies to defend themselves against pathogens and environmental stress. Among the mechanisms by which plants can control the pathogenic or environmental stress, the induction of metabolites acting as defence compounds is the most common feature. However, despite the knowledge about the effect of infection on the biological systems of plants, the metabolic changes related to it are still scarcely studied (Jahangir *et al.*, 2008).

Solanaceous plants, especially tomato (*Solanum lycopersicum*) provide an excellent model system to investigate plant–pathogen interactions. Also, tomato is one of the most popular vegetables worldwide from the agricultural point of view. However, this crop suffers from the attack of a number of pathogens including viruses, bacteria, fungi and nematodes. The study of the interaction of tomato plants with pathogens is important in order to establish effective methods to control pests (Arie *et al.*, 2007).

Citrus exocortis viroid (CEVd), the causal agent of the exocortis disease of citrus trees, produces a systemic compatible infection in Rutgers tomato plants consisting of plant stunting and an extreme leaf epinasty and rugosity (Conejero *et al.*, 1990). On the

other hand, *Pseudomonas syringae* causes a rapid tissue necrosis (hypersensitive response-like) of *S. lycopersicum* when injected at high concentration (Bellés *et al.*, 2006). In the present work a comparative analysis was applied to metabolic characterisation of the different responses of tomato plants against the two types of infections.

Metabolism is the end result of biochemical dynamics of living organisms starting with gene expression, and is therefore an essential part of a systems biology approach to study plant

\* Correspondence to: F. Maltese, Division of Pharmacognosy, Section Metabolomics, Institute of Biology, Leiden University, Leiden, The Netherlands. E-mail: f.maltese@chem.leidenuniv.nl

<sup>a</sup> Instituto de Biología Molecular y Celular de Plantas, Universidad Politécnica de Valencia–Consejo Superior de Investigaciones Científicas, Camino de Vera s/n 46022 Valencia, Spain

<sup>b</sup> Division of Pharmacognosy, Section Metabolomics, Institute of Biology, Leiden University, Leiden, The Netherlands

<sup>†</sup> This article is published in *Phytochemical Analysis* as a special issue on Metabolomics in Plant and Herbal Medicine Research, edited by Young Hae Choi, Hye Kyong Kim and Robert Verpoorte, all from Leiden University in the Netherlands.

defence. Different metabolic profiles are indicative of changes in metabolic pathways, thus, for example, enabling health and disease conditions in a system to be distinguished (Hankemeier, 2007). Comparing metabolic profiles of infected plants vs the corresponding controls is a powerful tool to unravel the biochemical pathways involved in multi-factorial disorders. Plants produce a huge number of metabolites which may largely differ in chemical characteristics. For this reason, a combination of methods to prepare and analyse samples is required. Thus, an extraction system and an instrumental technique must be carefully chosen to suit a particular biological question. Typical analytical equipment employed in metabolomics includes chromatographic methods [liquid chromatography (LC), gas chromatography (GC), capillary electrophoresis, and thin layer chromatography], mass spectrometry (MS) and nuclear magnetic resonance (NMR) spectroscopy (Verpoorte *et al.*, 2007).

In this study, a direct extraction method followed by NMR spectroscopy analysis in combination with multivariate data analysis was employed in order to investigate the metabolites associated with two different infections in tomato plants. Identification of metabolites responsible for the differences between control and infected samples can provide information about the chemical diversity of the signalling compounds involved in the defence response in plant–pathogen interaction.

## Experimental

### Plant material and inoculation procedure

Seeds from tomato (*Solanum lycopersicum* cv. Rutgers) (Western Hybrid Seeds Inc., CA, USA) were used in the experiments. The plants (one per pot) were grown in 15 cm-diameter pots containing a mixture of peat (Biolan) and vermiculite 1:1. The pots were subirrigated with a nutrient solution as described by Naranjo *et al.* (2003).

Infection of 5-week-old tomato plants with *P. syringae* pv. *tomato* was performed with a bacterial suspension obtained as follows: bacteria were grown overnight at 28°C in 20 mL Petri dishes with C3 agar medium (Oxoid, Basington, UK) supplemented with 0.45 g of  $\text{KH}_2\text{PO}_4$  per litre and 2.39 g of  $\text{Na}_2\text{HPO}_4 \cdot 12\text{H}_2\text{O}$  (pH 6.8) per litre. Bacterial colonies were then resuspended in 10 mM  $\text{MgSO}_4$  to a final concentration of  $\text{OD}_{600}$ : 0.1. Dilution plating was used to determine the final inoculum concentration, which averaged  $10^7$  cfu/mL. Two types of bacterial infections were carried out by infiltration and immersion. The bacterial infiltration procedure was as described in detail by Collinge *et al.* (1987). Briefly, aliquots of 100  $\mu\text{L}$  of this bacterial suspension were injected into the abaxial side of each leaflet (three to four panels per leaflet averaging 30 mm<sup>2</sup>) of the third and fourth leaf from the base of the plant with a 1 mL sterilised plastic syringe without needle. Equivalent control leaflets were mock-inoculated with 10 mM  $\text{MgSO}_4$ . The hypersensitive reaction consisted in the appearance of necrotic brown spots and cellular death in the inoculated leaf surface area 24 h after bacterial infiltration. Also, a strong epinasty of the inoculated leaves was evident at this time in response to the biotic stress (Zacarés *et al.*, 2007). For the bacterial immersion infection, the aerial portions of tomato plants were dipped in the suspension of bacteria ( $10^7$  cfu/mL) containing 10 mM  $\text{MgSO}_4$  and Silwet L-77 (0.05%) for 20 s, as described previously (Martin *et al.*, 1993). No symptoms were observed in these bacterial-treated plants when the samples were collected. For mock inoculations, plants were dipped in buffer with Silwet L-77 (0.025%) alone. The tomato plants were maintained in the greenhouse at 27 and 23°C (16 h day and 8 h night, respectively) and with relative humidity from 50 to 70%. Then the third and fourth leaves were harvested 48 h after bacterial infection by immersion or infiltration. The leaves were immediately frozen under liquid nitrogen, subsequently ground in a mortar and lyophilised. Three biological replicates were analysed for each treatment.

The inoculation procedure (Bellés *et al.*, 1991) of Rutgers tomato plants 8 days after sowing (cotyledon stage) with citrus exocortis viroid (CEVd) was performed by puncturing the stems of the seedlings with a needle dipped in either buffer or the 2 M LiCl-soluble fraction of nucleic acids from CEVd-infected tissue, as described previously (Semancik *et al.*, 1975). The control and infected tomato plants were placed in a controlled growth room at 30/25°C (16 h day/8 h night) with 70% relative humidity. Symptoms appeared 15–17 days after viroid infection. Control and infected tomato leaves were recollected 2 and 4 weeks after infection, frozen under liquid nitrogen, homogenised using precooled mortar and freeze-dried. Three biological replicates were analysed for each time.

### Extraction and NMR spectra measurements

Fifty milligrams of freeze-dried plant material were extracted in 2 mL Eppendorf tubes with 1.5 mL of a mixture of  $\text{KH}_2\text{PO}_4$  buffer (pH 6) in  $\text{D}_2\text{O}$  containing 0.05% trimethylsilyl propionic acid sodium salt (TMSP) and  $\text{CH}_3\text{OH}-d_4$  (1:1). The extracts were vortexed vigorously, sonicated for 20 min and then centrifuged at 13000 rpm for 10 min. Eight hundred microlitres of the supernatant was transferred in 5 mm NMR tubes for the spectral analysis.

<sup>1</sup>H-NMR, 2D-*J* resolved, <sup>1</sup>H–<sup>1</sup>H correlated spectroscopy (COSY), and heteronuclear multiple bonds coherence (HMBC) spectra were recorded at 25°C on a 600 MHz Bruker AV 600 spectrometer equipped with cryoprobe operating at a proton NMR frequency of 600.13 MHz. Methyl signals of  $\text{CH}_3\text{OH}-d_4$  were used as the internal lock. Each <sup>1</sup>H NMR spectrum consisted of 128 scans requiring 10 min acquisition time with the following parameters: 0.25 Hz/point, pulse width (PW) = 30° (10.8  $\mu\text{s}$ ), and relaxation delay (RD) = 1.5 s. A presaturation sequence was used to suppress the residual  $\text{H}_2\text{O}$  signal with low power selective irradiation at the  $\text{H}_2\text{O}$  frequency during the recycle delay. FIDs were Fourier transformed with LB = 0.3 Hz and the spectra were zero-filled to 32 K points. The resulting spectra were manually phased and baseline-corrected, and calibrated to TMSP at 0.0 ppm, using Topspin (version 2.1, Bruker). All the 2D NMR parameters were the same as in our previous reports (Jahangir *et al.*, 2008).

### Data analysis

<sup>1</sup>H NMR spectra were automatically reduced to ASCII files using AMIX (version 3.7, Bruker Biospin). Spectral intensities were scaled to total intensity TMSP and reduced to integrated regions of equal width (0.04 ppm) corresponding to the region of  $\delta$  0.4–10.00. The region of  $\delta$  4.7–4.9 was excluded from the analysis because of the residual signal of water as well as  $\delta$  3.28–3.34 for residual methanol. Principal component analysis (PCA) and partial least square-discriminant analysis (PLS-DA) were performed with the SIMCA-P software (version 11.0, Umetrics, Umeå, Sweden) using Pareto or unit variance (UV) scaling method.

### Extraction and LC-MS analysis

Leaflets (0.5 g fresh weight) of tissue were ground with a pestle in a mortar using liquid nitrogen, then homogenised in 1.5 mL of 90% methanol. The extracts were vortexed vigorously, sonicated for 15 min and then centrifuged at 14000 *g* for 15 min using 2 mL Eppendorf tubes to remove cellular debris. The supernatant (1.5 mL) was dried at 35°C under a flow of nitrogen. The residue was resuspended in 100  $\mu\text{L}$  of methanol and filtered through 0.45  $\mu\text{m}$  Sparton 13/0.45RC filters (Schleicher & Schuell, Keene, NH, USA) nylon filters (Waters, Millford, MA, USA). The samples were analysed in electrospray ionisation (ESI)-MS using a 1515 Waters HPLC binary pump, a 996 Waters photodiode detector (range of maxplot between 240 and 400 nm, spectral resolution of 1.2 nm), and a ZMD Waters single quadrupole mass spectrometer ESI ion source. The source parameters of the mass spectrometer for ESI in positive mode were the following: capillary voltage 2500 V, cone voltage 20 V, extractor 5 V, RF Lens 0.5 V, source block temperature 100°C and desolvation gas temperature 300°C. The desolvation and cone gas used was nitrogen at a flow of

400 and 60 L per min, respectively. The ESI data acquisition was in the conditions of a full-scan range from mass-to-charge ratio ( $m/z$ ) 100 to 700 at 1 s per scan. Filtered samples (20  $\mu$ L) from methanolic extracts were injected at room temperature into a reverse-phase SunFire 5  $\mu$ m  $C_{18}$  (4.6  $\times$  150 mm; Waters) column. A 20 min linear gradient of 1% (v/v) acetic acid (J. T. Baker, Phillipsburg, NJ, USA) in Milli Q water to 100% methanol (J. T. Baker) at a flow rate of 1.0 mL/min was applied. A post-column split delivered approximately 25% of the flow to the mass spectrometer and the rest to the PDA detector. Mass and UV-absorption spectra were obtained using the Masslynx Waters software.

## Results and Discussion

To investigate the metabolites involved in tomato–pathogen interactions, Rutgers tomato plants were infected with CEVd or *P. syringae* pv. *tomato* and the metabolic changes were analysed by NMR spectroscopy. For bacterial infection of *P. syringae* pv. *tomato*, two different infection methods, either infiltration or

immersion, were performed on 5-week-old plants and metabolic analysis was carried out 48 h after infection of the plants. However, in the case of viroid infection, 8-day-old plants were used because it is known that viroid infection is effective at cotyledon stage of Rutgers tomato plants (Granell *et al.*, 1987), and samples were collected 2 and 4 weeks after infection.

A large number of primary and secondary metabolites were identified in the  $^1\text{H}$  NMR and 2D  $J$ -resolved spectra with assistance of 2D-NMR techniques including  $^1\text{H}$ - $^1\text{H}$  COSY and HMBC. The NMR data (chemical shifts and coupling constants) of the identified metabolites are listed in Table 1. All the signals were assigned and confirmed using an in-house-built database of NMR spectra of natural products from plants.

In the amino acid region ( $\delta$ 0.8–4.0) alanine, glycine, isoleucine, threonine and valine were identified. Organic acids such as acetic, aspartic, citric, glutamic, glyceric, malic and GABA ( $\gamma$ -amino-butyric acid) as well as choline and the signals of linoleic acid were identified. For sugars, resonances for  $\beta$ -glucose,

**Table 1.**  $^1\text{H}$  chemical shifts ( $\delta$ ) and coupling constants (Hz) of control and infected *S. lycopersicum* leaves detected from 1D and 2D NMR spectra in 50% MeOH- $d_4$  in  $\text{D}_2\text{O}$  ( $\text{KH}_2\text{PO}_4$  buffer pH 6.0)

Metabolite	Chemical shifts (ppm) and coupling constants (Hz)
Linoleic acid	0.96 (t, $J = 7.5$ Hz), 1.30 (brs)
Valine	1.01 (d, $J = 7.0$ Hz), 1.06 (d, $J = 7.0$ Hz)
Isoleucine	1.02 (d, $J = 7.0$ Hz)
Threonine	1.33 (d, $J = 6.6$ Hz)
Alanine	1.48 (d, $J = 7.2$ Hz),
GABA	1.90 (m), 2.31 (t, $J = 7.2$ Hz), 3.01 (t, $J = 7.2$ Hz)
Acetic acid	1.94 (s)
Glutamic acid	2.42(m), 2.13 (m), 2.05 (m)
Malic acid	4.29 (dd, $J = 8.3, 3.9$ Hz), 2.72 (dd, $J = 15.8, 3.9$ Hz), 2.47 (dd, $J = 15.8, 8.3$ Hz)
Citric acid	2.71 (d, $J = 16.3$ Hz), 2.53 (d, $J = 16.3$ Hz)
Aspartic acid	2.81 (dd, $J = 17.4, 3.5$ Hz), 2.65 (dd, $J = 17.4, 9.3$ Hz)
Ethanolamine	3.12 (t, 5.5 Hz)
Choline	3.21 (s)
Glycine	3.51 (s)
Inositol	3.61 (t, $J = 9.9$ Hz), 3.47 (dd, $J = 9.9, 2.8$ Hz), 3.24 (t, $J = 9.4$ Hz)
Glyceric acid	4.01 (dd, $J = 5.9, 2.6$ Hz), 3.80 (dd, $J = 12.1, 2.6$ Hz)
Sucrose	5.40 (d, $J = 3.8$ Hz), 4.17 (d, $J = 8.7$ Hz)
$\beta$ -glucose	4.58 (d, $J = 7.9$ Hz)
$\alpha$ -glucose	5.18 (d, $J = 3.7$ Hz)
Rhamnose in rutin	1.09 (d, $J = 6.1$ Hz)
Fumaric acid	6.54 (s)
Tyrosine	6.91 (d, $J = 8.0$ Hz)
Phenylalanine	7.33 (m), 3.93 (dd, $J = 8, 4$ Hz)
Formic acid	8.46 (s)
Ferulic acid glucoside	7.66 (d, $J = 16.0$ Hz), 7.18 (d, $J = 2.0$ Hz), 7.10 (dd, $J = 8.2, 2.0$ Hz), 6.89 (d, $J = 8.2$ Hz), 6.47 (d, $J = 16.0$ Hz), 5.10 (d, $J = 4.9$ Hz),
Ferulic acid	7.63 (d, $J = 15.9$ Hz), 7.16 (d, $J = 2.0$ Hz), 7.06 (dd, $J = 8.2, 2.0$ Hz), 6.87 (d, $J = 8.2$ Hz), 6.40 (d, $J = 16.0$ Hz)
Caffeic acid	7.64 (d, $J = 15.9$ Hz), 7.16 (d, $J = 2.0$ Hz), 7.07 (dd, $J = 8.2, 2.0$ Hz), 6.86 (d, $J = 8.2$ Hz), 6.39 (d, $J = 16.0$ Hz)
Chlorogenic acid	7.61 (d, $J = 15.9$ Hz), 6.37 (d, $J = 15.9$ Hz), 7.15 (d, $J = 2.0$ Hz), 7.05 (dd, $J = 8.2, 2.0$ Hz), 6.86 (d, $J = 8.2$ Hz), 5.33 (td, $J = 10.0, 4.8$ Hz),
Rutin	6.99 (d, $J = 8.4$ Hz), 6.54 (d, $J = 2.0$ Hz), 6.32 (d, $J = 2.0$ Hz), 7.68 (d, $J = 2.0$ Hz), 7.63 (dd, $J = 8.4, 2.0$ Hz), 5.02 (d, $J = 7.9$ Hz)
Gentisic acid glycosylated	7.52 (d, $J = 3.0$ Hz), 7.12 (dd, $J = 8.8, 3.0$ Hz), 6.84 (d, $J = 8.8$ Hz), 5.04 (d, $J = 7.8$ Hz)
Adenosin	5.96 (d, $J = 4.0$ Hz), 8.24 (s), 8.54 (s)
Trigonelline	9.14 (s), 8.87 (m), 8.10 (dd, $J = 7.5, 6.5$ Hz)

$\alpha$ -glucose, sucrose, rhamnose and fructose were assigned. Also, a sugar alcohol, inositol was found to be present in the extract. This was confirmed by the fact that H-4 ( $\delta$  3.61) of inositol correlated with H-5 ( $\delta$  3.24) and H-3 ( $\delta$  3.47) in the COSY spectrum.

Most of  $^1\text{H}$  NMR signals in the aromatic region ( $\delta$  6.0–8.5) belong to secondary metabolites. The presence of four doublets with the same coupling constant ( $d, J = 16.0$  Hz) in the range of  $\delta$  6.35–6.52 indicated the presence of the *trans* olefinic protons of the phenylpropanoids. The  $^1\text{H}$ – $^1\text{H}$  COSY correlation observed with protons at  $\delta$  7.60–7.70 ( $d, J = 16.0$  Hz) and the coupling with carbonyl carbons at  $\delta$  171 in HMBC spectrum confirmed a phenylpropanoid moiety. A flavonoid glycoside, rutin was detected. The signals at  $\delta$  6.32 and 6.54 correlated with a *meta* coupling constant ( $J = 2.0$  Hz) in the COSY spectrum were assigned as H-6 and H-8 of quercetin moiety from rutin, respectively. The correlations between the signals at  $\delta$  6.99 of H-5' ( $d, J = 8.4$  Hz) and  $\delta$  7.63 of H-6' ( $dd, J = 8.4, 2.0$  Hz) and the presence of H-2' at  $\delta$  7.68 ( $d, J = 2.0$  Hz) led to elucidation of the B-ring protons of the flavonoid. The anomeric protons of rutin was detected at  $\delta$  5.02 ( $\beta$ -glucosyl,  $d, J = 7.9$  Hz) and  $\delta$  4.54 ( $\alpha$ -rhamnosyl,  $d, J = 1.5$  Hz). In the HMBC spectrum, the  $\beta$ -glucosyl proton correlates with C-3 at  $\delta$  133.6. Also, the H-6 of rhamnose of rutin was detected at  $\delta$  1.09. The identification of rutin was further confirmed by the presence of a peak ( $t_r = 12.23$  min) with  $m/z$  609.3  $[\text{M} - \text{H}]^-$  in the LC-MS chromatograms of tomato leaves methanolic extracts. This compound was coeluted and had identical UV and mass spectra to that of the standard compound.

To deal with the large number of  $^1\text{H}$  NMR data, multivariate data analysis was employed. From the diverse multivariate handling techniques principal component analysis (PCA) was first used to identify metabolic changes after viroid and bacterial infection of Rutgers plants. No clear separation of bacterial or viroid infected plants from their respective controls was observed in the PCA score plot (Fig. 1). Instead, the separation between two experimental conditions was clearly observed. This might be due to the fact that the effect of different growing conditions between both experiments was bigger than the infection itself. One of the distinguishable growing conditions is temperature. We used different temperature conditions for the sample because a photoperiod of 30°C/25°C was necessary for successful viroid

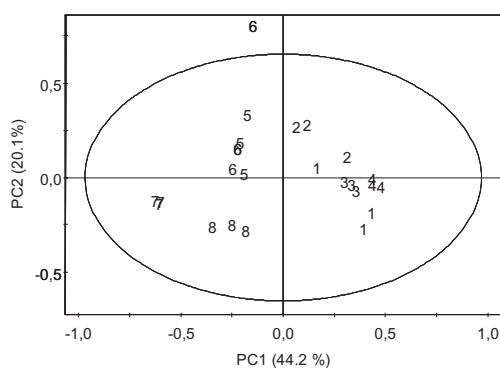


**Figure 1.** Score plot of PCA based on whole range of the  $^1\text{H}$  NMR signals in the range of  $\delta$  0.3–10.0. 1: Control for bacterial infection (infiltration); 2: Rutgers tomato infected by *Pseudomonas syringae* by infiltration; 3: control for bacterial infection (immersion); 4: Rutgers tomato infected by *Pseudomonas syringae* by immersion; 5: control for viroid infection (2 weeks); 6: Rutgers tomato infected by CEVd 2 weeks; 7: control for viroid infection (4 weeks); 8: Rutgers tomato infected by CEVd 4 weeks.

infection but 27°C/23°C was the right one for bacterial infection. This temperature variation could explain the discrimination of two groups in PC1. For the investigation of differentiating metabolites affected by temperature conditions, a loading plot was used to correlate the different groups with the corresponding metabolites. All the tomato plants grown at high temperatures were correlated with elevated levels of gentisic acid, sucrose, inositol, GABA, threonine, valine and linoleic acid. On the other hand the plants cultivated at 27°C/23°C temperatures showed higher concentrations of phenylpropanoids, rutin, glucose, aspartate, glutamate, citrate, malate and alanine. However, there are many unknown factors in growing conditions. The exact factor to affect the metabolic change should be further studied.

A large discrimination between infected and control plants was observed in PCA when the two types of plant–pathogen interactions were analysed separately (Figs 2 and 3). In particular a clear separation in PCA was shown between Rutgers infected with *Pseudomonas* by infiltration and control plants (Fig. 2). Nevertheless, after 48 h from bacterial immersion there were no significant changes in the metabolomic profile of plants compared to control. This is in agreement with previous reports on bacterial-infected tomato leaves (Lund *et al.*, 1998; Ciardi *et al.*, 2000; O'Donnell *et al.*, 2001), in which the plant response occurred during later stages of the infection when compared with the rapid hypersensitive-like response of the leaves after inoculation by infiltration with high doses of bacteria. In this case, for the identification of the metabolites induced in the hypersensitive interaction with bacteria, the loading plot of PC1 was analysed (Fig 2). High concentrations of amino acids, organic acids, rutin and phenylpropanoids were characteristic of bacteria-infected plants by infiltration. Also, the  $^1\text{H}$  NMR signal at  $\delta$  5.17 ( $d, J = 3.0$  Hz) was clearly increased and probably belonged to a sugar derivative. This class of compounds has already been found to have an important defensive role against insects in many *Solanaceae* species (Slocombe *et al.*, 2008). Only alanine, malic acid, inositol and glucose were at higher levels in the control plants. This increase of primary and secondary metabolism upon bacterial infection suggests that *Pseudomonas syringae* in tomato leaves could cause an induced systemic resistance (ISR) as described by Jahangir and co-workers in infected *Brassica* leaves by different bacteria (Jahangir *et al.*, 2008). The decreased level of sugars is a typical indication of the alteration of carbohydrates metabolism following infection (Abdel-Farid *et al.*, 2009). Part of

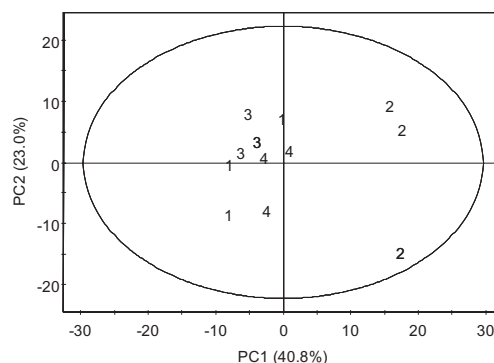


**Figure 2.** Score plot of PCA, from Rutgers tomato plants infected with *P. syringae*, based on whole range of the  $^1\text{H}$  NMR signals in the range of  $\delta$  0.3–10.0. Numbers of the samples are the same than in Fig. 1.

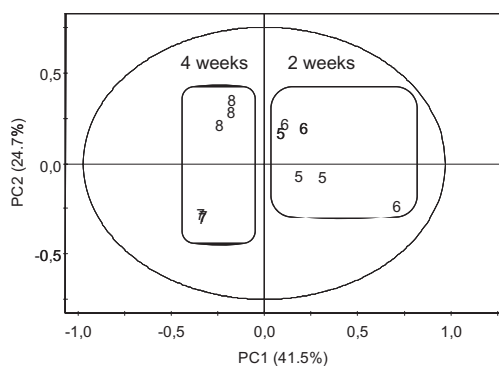


**Figure 3.** Score plot of PCA, from Rutgers tomato plants infected with CEVd, based on whole range of the  $^1\text{H}$  NMR signals in the range of  $\delta$  0.3–10.0. Numbers of the samples are the same than in Fig. 1.

the sugars is involved in energy generation and part is implicated as precursors in the secondary metabolite biosynthesis, as shown by the increased level of flavonoids and phenylpropanoids known to have a generic defensive role in the response of plants against bacterial attack (Treutter, 2006; Tan *et al.*, 2004). In fact, an accumulation of *p*-coumaric, caffeic and ferulic acids mainly forming esters with glucose has been observed in other plant–pathogen systems such as *Cucumis sativus* and *Cucumis melo* infected with prunus necrotic ringspot virus (PNRSV) or melon necrotic spot virus (MNSV), respectively (Bellés *et al.*, 2008).

To investigate the metabolites characterising the CEVd infected compared with the control plants, the loading plot of PC2 was analysed in the PCA performed by only this systematic interaction (Fig. 3). In contrast to bacterial infection, only a few primary metabolites were induced by the viroid infection such as glucose and malic acid. In the aromatic region, high concentrations of gentisic acid glycoside were characteristic of viroid-infected plants. The increased signals in the  $^1\text{H}$  NMR spectrum at  $\delta$  7.52 (d,  $J = 3.0$  Hz), 7.12 (dd,  $J = 8.8, 3.0$  ppm) and 6.84 (d,  $J = 8.8$  Hz), coupled between each other in the  $^1\text{H}$ – $^1\text{H}$  COSY spectrum, indicate the presence of the phenolic compound. The upfield shift of the phenolic protons, in comparison with those of the reference compound gentisic acid ( $\delta$  7.30, 7.01 and 6.82), confirmed that the compound was accumulated in a glycosylated form. Gentisic acid (GA) has been described as additional to salicylic acid pathogen-inducible signal of plant defences in tomato (Bellés *et al.*, 1999). GA has also been reported in the literature to be induced to high levels in systemic, non-necrotising infections as CEVd and ToMV infected tomato plants, but not in those plants infected with the necrotising pathogen *Pseudomonas syringae* (Bellés *et al.*, 1999). In addition, in other compatible plant–pathogen interaction systems such as *Cucumis sativus* and *Gynura aurantiaca* infected with either prunus necrotic ringspot virus (PNRSV) or CEVd, respectively, GA was accumulated and thus associated with these systemic infections (Bellés *et al.*, 2006). In plants, phenolic acids are mostly present in the glucosylated form, but in a previous report GA was demonstrated to be conjugated to xylose (Fayos *et al.*, 2006). Here, for analysing GA-glycoside, we followed the same protocol described previously in detail (Fayos *et al.*, 2006). LC-MS chromatograms of infected CEVd plants confirmed the induction of GA-xyloside by the presence of a peak ( $t_r = 9.64$  min) whose mass spectrum showed a molecular ion  $[\text{M} - \text{H}]^- m/z$  285.2 and an ion fragmentation: [gentisic acid – H] $^- m/z$  153.1 and [gentisic acid – COOH] $^- m/z$  108 by electrospray

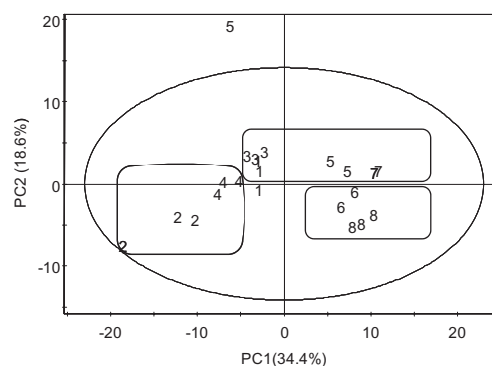


**Figure 4.** Score plot of PLS-DA based on the  $^1\text{H}$  NMR signals in the range of  $\delta$  0.3–10.0. Numbers of the samples are the same as in Fig. 1.

ionisation negative ion mode. In addition, this peak also coeluted with authentic standard GA 5-*O*- $\beta$ -D-xylopyranoside under different conditions of HPLC eluent. Unambiguous identification of the glycoside was achieved through the structural elucidation of the sugar joined to GA by acid hydrolysis of the compound and analysis of the carbohydrate in a pulsed electrochemical detector by spiking with xylose (data not shown). The metabolic changes in time during the viroid infection were investigated by principal component analysis of the NMR spectra at early (2 weeks) and late (4 weeks) stages. The loading plot of PC1 revealed that the secondary metabolites were more accumulated in the samples two weeks after infection (Fig. 3).

Metabolomic analysis was concluded by doing the partial least square-discriminant analysis. Three discrete classes, control, bacteria and viroid-infected plants, were created for this supervised multivariate data analysis. Results are shown in Fig. 4. The loading plot of PLS-DA confirmed the results obtained with PCA, as already discussed.

Interestingly, the induced metabolites are different from each other depending on the infection source, bacteria or viroid. A wide range of primary and secondary compounds could be identified using NMR after a simple extraction and correlated with the different plant microbe interaction systems after multivariate data analysis. In conclusion, the analytical techniques used in this study have greatly expanded the range of metabolites previously found in response to pathogen exposure (Bellés *et al.* 1999, 2006, 2008). Thus, our work may help to identify metabolites involved in compatible and incompatible pathogen interactions that might have some role in tomato plant defence.

### Acknowledgements

We gratefully acknowledge Cristina Torres for the technical support. This work has been supported by grant BFU2006-11546 and fellowship JC2008-00432 (to M.P.L.G) from Spanish Ministry Science and Innovation.

### References

- Abdel-Farid IB, Jahangir M, van den Hondel CAMJ, Kim HK, Choi YH, Verpoorte R. 2009. Fungal infection-induced metabolites in *Brassica rapa*. *Plant Sci* **176**: 608–615.
- Arie T, Takahashi H, Kodama M, Teraoka T. 2007. Tomato as a model plant for plant–pathogen interactions. *Plant Biotechnol* **24**: 135–147.

- Bellés JM, Carbonell J, Conejero V. 1991. Polyamines in plants infected by citrus-exocortis viroid or treated with silver ions and ethephon. *Plant Physiol* **96**: 1053–1059.
- Bellés JM, Garro R, Fayos J, Navarro P, Primo J, Conejero V. 1999. Gentisic acid as a pathogen-inducible signal, additional to salicylic acid for activation of plant defenses in tomato. *Mol Plant–Microbe Interact* **12**: 227–235.
- Bellés JM, Garro R, Pallas V, Fayos J, Rodrigo I, Conejero V. 2006. Accumulation of gentisic acid as associated with systemic infections but not with the hypersensitive response in plant–pathogen interactions. *Planta* **223**: 500–511.
- Bellés JM, Lopez-Gresa MP, Fayos J, Pallas V, Rodrigo I, Conejero V. 2008. Induction of cinnamate 4-hydroxylase and phenylpropanoids in virus-infected cucumber and melon plants. *Plant Sci* **174**: 524–533.
- Ciardi JA, Tieman DM, Lund ST, Jones JB, Stall RE, Klee HJ. 2000. Response to *Xanthomonas campestris* pv. vesicatoria in tomato involves regulation of ethylene receptor gene expression. *Plant Physiol* **123**: 81–92.
- Collinge DB, Milligan DE, Dow JM, Scofield G, Daniels MJ. 1987. Gene-expression in *Brassica campestris* showing a hypersensitive response to the incompatible pathogen *Xanthomonas campestris* pv. vitians. *Plant Mol Biol* **8**: 405–414.
- Conejero V, Bellés JM, García-Breijo F, Garro R, Hernández-Yago J, Rodrigo I, Vera P. 1990. Signalling in viroid pathogenesis. In *Recognition and Response in Plant–Virus Interactions*, Fraser RSS (ed.). Springer: Berlin; 233–261.
- Fayos J, Bellés JM, López-Gresa MP, Primo J, Conejero V. 2006. Induction of gentisic acid 5-O-beta-D-xylopyranoside in tomato and cucumber plants infected by different pathogens. *Phytochemistry* **67**: 142–148.
- Granell A, Bellés JM, Conejero V. 1987. Induction of pathogenesis-related proteins in tomato by citrus exocortis viroid, silver ion and ethephon. *Physiol Mol Plant Pathol* **31**: 83–90.
- Hankemeier T. 2007. Medical system biology. In *Abstracts Book. The 11th International Congress, Phytopharm*. Leiden, The Netherlands; 20.
- Jahangir M, Kim HK, Choi YH, Verpoorte R. 2008. Metabolomic response of *Brassica rapa* submitted to pre-harvest bacterial contamination. *Food Chem* **107**: 362–368.
- Lund ST, Stall RE, Klee HJ. 1998. Ethylene regulates the susceptible response to pathogen infection in tomato. *Plant Cell* **10**: 371–382.
- Martin GB, Brommonschenkel SH, Chunwongse J, Frary A, Ganai MW, Spivey R, Wu TY, Earle ED, Tanksley SD. 1993. Map-based cloning of a protein-kinase gene conferring disease resistance in tomato. *Science* **262**: 1432–1436.
- Mehta A, Brasileiro ACM, Souza DSL, Romano E, Campos MA, Grossi-De-Sa MF, Silva MS, Franco OL, Fragoso RR, Bevilieri R, Rocha TL. 2008. Plant–pathogen interactions: what is proteomics telling us? *FEBS J* **275**: 3731–3746.
- Naranjo MA, Romero C, Bellés JM, Montesinos C, Vicente O, Serrano R. 2003. Lithium treatment induces a hypersensitive-like response in tobacco. *Planta* **217**: 417–424.
- O'Donnell PJ, Jones JB, Antoine FR, Ciardi J, Klee HJ. 2001. Ethylene-dependent salicylic acid regulates an expanded cell death response to a plant pathogen. *Plant J* **25**: 315–323.
- Semancik JS, Morris TJ, Weathers LG, Roderf BF, Kearns DR. 1975. Physical-properties of a minimal infectious RNA (viroid) associated with exocortis disease. *Virology* **63**: 160–167.
- Slocombe SP, Schauvinhold I, McQuinn RP, Besser K, Welsby NA, Harper A, Aziz N, Li Y, Larson TR, Giovannoni J, Dixon RA, Broun P. 2008. Transcriptomic and reverse genetic analyses of branched-chain fatty acid and acyl sugar production in *Solanum pennellii* and *Nicotiana benthamiana*. *Plant Physiol* **148**: 1830–1846.
- Tan JW, Bednarek P, Liu HK, Schneider B, Svatos A, Hahlbrock K. 2004. Universally occurring phenylpropanoid and species-specific indolic metabolites in infected and uninfected *Arabidopsis thaliana* roots and leaves. *Phytochemistry* **65**: 691–699.
- Treutter D. 2006. Significance of flavonoids in plant resistance: a review. *Environ Chem Lett* **4**: 147–157.
- Verpoorte R, Choi YH, Kim HK. 2007. NMR-based metabolomics at work in phytochemistry. *Phytochem Rev* **6**: 3–14.
- Zacarés L, López-Gresa MP, Fayos J, Primo J, Bellés JM, Conejero V. 2007. Induction of *p*-coumaroyldopamine and feruloyldopamine, two novel metabolites, in tomato by the bacterial pathogen *Pseudomonas syringae*. *Mol Plant–Microbe Interact* **20**: 1439–1448.